Effect of Preweld and Postweld Heat Treatment on the Properties of GTA Welds in Ti-6Al-4V Sheet

Optimum welding parameters are determined for joining thin titanium sheets

BY G. THOMAS, V. RAMACHANDRA, M. J. NAIR, K. V. NAGARAJAN, AND R. VASUDEVAN

ABSTRACT. Ti-6Al-4V is being used as a potential candidate material for critical components in satellite and launch vehicles at very high stress levels. The requirement of sound and reliable welds in these components is imperative. This paper describes the GTA welding studies carried out on 2.6-mm-thick Ti-6Al-4V sheet. Through a series of bead-on-plate and groove welds conducted on pairs of 60 X 50 X 2.6-mm pieces, an optimum weld schedule was determined. The effect of preweld and postweld heat treatments on the mechanical properties and microstructure of the weldment are also discussed in detail.

Introduction

Titanium and its alloys possess outstanding strength-to-weight ratios at temperatures in the range of –253° (liquid hydrogen) to 500°C (–420° to 932°F) and good corrosion resistance to most fuels and oxidizers as well as to the general atmosphere. The above advantages, accompanied by good fracture toughness, fatigue resistance and a high stiffness-to-weight ratio (buckling resistance) make titanium and its alloys an important class of materials for aerospace applications.

Ti-6Al-4V, the most important aerospace titanium alloy, is extensively used (Ref. 1) in rockets, missiles and space craft as pressure vessels, propellant tanks, upper stage motor cases and fasteners. The Indian space program is also using Ti-6Al-4V for gas bottles and propellant tanks in its launch vehicles and satellites. Welding is important in the fabrication of these components. The materials and metallurgy group of the Vikram Sarabhai Space Center, therefore, initiated welding studies of 2.6-mm (0.10-in.) Ti-6Al-4V sheet with a purpose to: 1) optimize the GTA welding parameters to get a sound weld, and 2) study the effect of preweld and postweld heat treatments on the mechanical properties of the optimized welds.

G. THOMAS, V. RAMACHANDRA, M. J. NAIR and K. V. NAGARAJAN are with Vikram Sarabhai Space Center, Trivandrum, India. R. VASUDEVAN is a Professor in the Department of Metallurgy, Indian Institute of Technology, Madras, India.

KEY WORDS

GTAW
Ti-6Al-4V Alloy
Microstructure
Heat Treatment
Satellite Components
Mechanical Properties
Aerospace Applications
Titanium Alloy
Radiographic Analysis
Hardness

Experimental Procedure

Material

Welding was carried out on pairs of 60 X 50 X 2.6-mm (2.4 X 2 X 0.10-in.) pieces cut from 2.6 mm Ti-6Al-4V mill-annealed sheets.

Welding

The main difference between the GTA welding of titanium base alloys and less reactive metals and alloys is that the atmospheric gases are absorbed not only by the molten weld pool, but also by any part of the solid titanium that is heated to temperatures above 600°C (1112°F), with the rate of absorption increasing rapidly with temperature. This reactivity requires an effective arrangement for shielding a sizable area of the workpiece, and it was achieved in this experiment with the use of the fixture shown in Fig.1. The inert gas flowing out through the perforations in the backup plate and the clamping pads provided sufficient shielding to the workpiece.

A manual GTA torch in conjunction with a 400-A DC power supply was used for welding. Argon gas was used for shielding in the torch, trailer, clamp pad and back-up plate.

Strips of 2.5 X 2.6 X 200 mm (0.01 X 0.01 X 8 in.) titanium were cut from the Ti-6Al-4V sheet and used as filler metal. Both the filler metal strips and the workpieces were thoroughly cleaned with a wire brush and emery paper, pickled in $H_2O/HNO_3/HF$ solution (Ref. 2) (76/20/4 vol-%) , and then degreased with acetone prior to welding. A preliminary series of bead-on-plate welds were made by varying the current, travel speed, electrode-to-work distance and gas flow rates. Based on the shape and surface conditions of these beads, a set of parameters was selected. Subsequently, a number of single-pass, square-groove welds were made from pairs of 60 X 50 X 2.6 mm pieces by varying the root opening and filler metal feed rate, as well as the initially selected parameters. The best welding conditions were arrived at by examining the top and bottom bead surfaces and studying the internal soundness through radiographic analysis.

Heat Treatment

In order to study the effects of preweld and postweld heat treatments on the weldment structure and the mechanical properties, the following combinations were utilized:

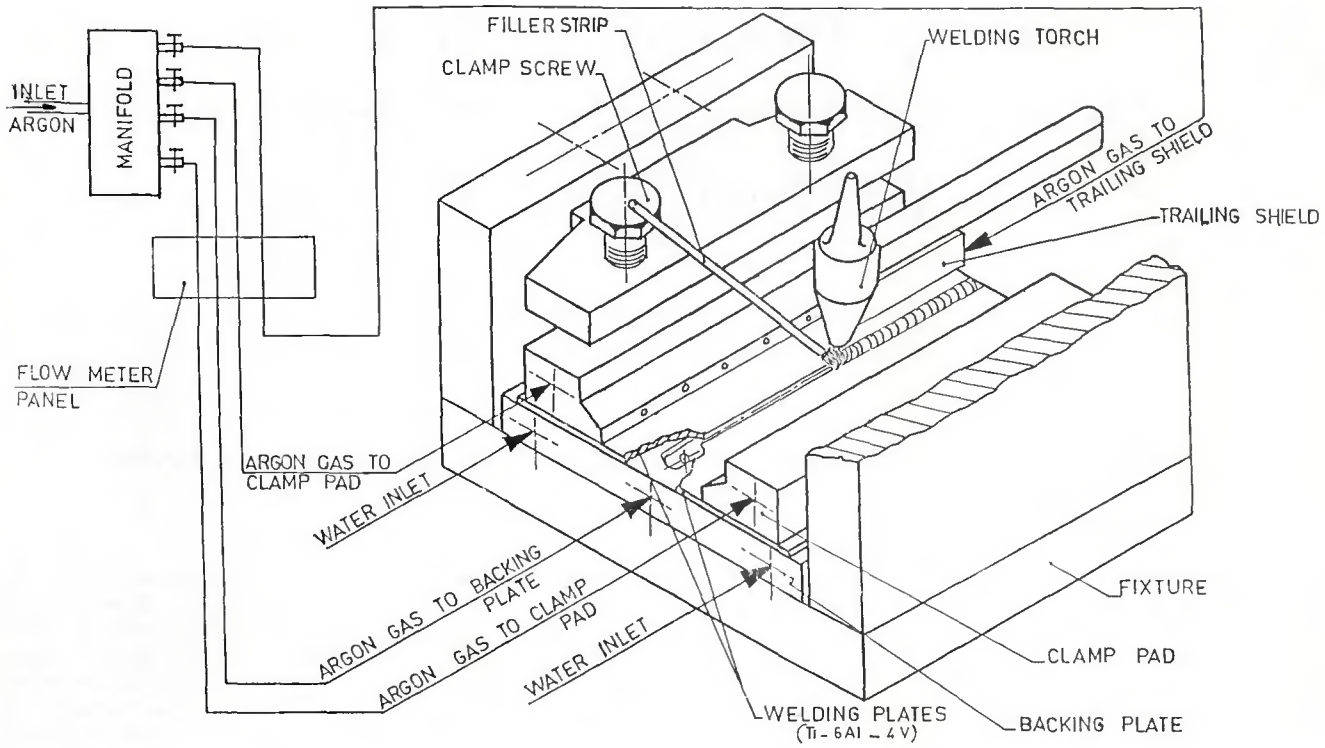

Fig. 1 — Welding fixture.

1) As-received, welded and stress relieved.

2) As-received, welded, solution treated and aged.

3) As-received, solution treated, welded and aged.

4) As-received, solution treated and aged, welded and stress relieved.

The stress relieving and aging treatments were carried out at 600° and 540°C (1112° and 1004°F), respectively, for 1 h, followed by air cooling. In the case of solution treatment at 950°C (1742°F) for half an hour followed by water quenching, the samples were vacuum sealed in an ordinary glass tube, which melted and gave a protective coating to the samples at high temperatures. All samples were ground to remove the thin oxide layer or glass coating on the surface.

Table 1—Manual GTA Welding Schedule

Sheet Preparation	Edges sheared, milled, ground and degreased
Filler strip size	2.6 × 2.5 × 200 mm
Electrode	2.4-mm-diameter 2% Thoriated Tungsten
Polarity	Straight
Type of weld	Single pass
Joint preparation	Square butt
Weld gap	1 mm
Current	125–130 A
Voltage	16–20 V
Electrode-to-work distance	2–3 mm
Filler strip feed	3–4 mm per minute
Weld speed	75–80 mm per minute
Torch inert gas	0.3–0.4 m^3 per hour
Trailer inert gas	0.2 m^3 per hour
Backup inert gas	0.15 m^3 per hour
Purge inert gas	0.15 m^3 per hour

Sample Preparation and Testing

All welded samples were visually inspected and tested with dye penetrant for surface defects. They were also radiographed for internal soundness. From the radiographically sound samples, tensile samples were prepared with the weld oriented transverse to the gauge length, as shown in Fig. 2. The tensile samples were tested on an Instron testing machine at a strain rate of 25 X 10^{-2}/min.

Samples were prepared from the welded pieces and hardness measurements were made at regular intervals using a Rockwell C scale across the composite weld structure from base metal on one side to base metal on the other side. For metallographic studies, samples were prepared using a standard metallographic method. Kroll's reagent was used for etching the samples and the microstructure of the base metal (BM), the heat-affected zone (HAZ) and the fusion zone (FZ) were observed in an optical microscope.

Results and Discussion

Determination of Welding Parameters

The welding parameters optimized for the 2.6-mm-thick Ti-6Al-4V sheet are given in Table 1. Some of the important process variables that have considerable effect on depth of penetration, bead shape and weld soundness are as follows:

1) Arc voltage
2) Welding current
3) Travel speed
4) Electrode-to-work distance
5) Root opening
6) Electrode shape
7) Filler metal feed rate
8) Shielding gas flow rate
9) Cleanliness

All of the above parameters except the arc voltage can be independently varied. The arc voltage does not remain constant as it increases or falls during welding due to arc characteristics. The arc voltage in general varies with welding current and the distance between the tip of the electrode and the base metal surface.

The welding current was found to have a significant effect on increasing the depth of penetration. However, when the welding current was increased beyond a certain value, the surface conditions of the weld bead became unsatisfactory. This indicated that for a given sheet thickness, there exists a maximum limiting current that gives the deepest penetration with a good bead surface. For 2.6-mm-thick Ti-6Al-4V sheet, this limiting current was found to be 125 to 130 A.

The effect of travel speed on depth of penetration is relatively less as compared to welding current. The depth of

penetration varies inversely with travel speed and a large change in travel speed was required to bring about any appreciable change in depth of penetration. Increasing the weld speed beyond a certain critical limit produced a deterioration of the weld, resulting in undercutting or humping. In the present study, a travel speed of 75 to 90 mm/min (2.9 to 3.5 in./min.) was found to produce a satisfactory weld for a given current of 125 to 130 A. This travel speed was also found to be high enough to keep the heat input level to the minimum required without sacrificing good inert gas shielding.

The electrode-to-work distance was also found to have an influence on the acceptability of the bead surface. A larger distance between the tip of the electrode and the sheet surface caused turbulence to occur in the weld pool. A shorter distance, on the other hand, produced an undercut condition. In the present case, a distance of 2 to 3 mm (0.8 to 0.12 in.) maintained manually between the electrode tip and the sheet surface produced a weld free of undercutting and humping.

Although the blunted electrode shape was found to produce deeper and more narrow welds, the arc had a tendency to wander. Therefore, pointed electrodes are more practical. A smaller root opening and a low filler metal feed rate were found to cause insufficient weld penetration. On the contrary, a large root opening and a high filler metal feed rate gave a wider FZ and HAZ and produced weld porosity. A root opening of 1 mm (0.04 in.) and a filler metal feed rate of 3 to 4 mm/min produced sound welds. The golden yellow to dark blue colors obtained on the weld surface were removed in the subsequent trials by altering the gas flow rates through the torch, clamping pads, backup plate and trailing shield. The optimized inert gas flow rates, which gave a bright metallic weld surface, confirmed the adequacy of the inert gas protection achieved through the use of special fixtures.

Cleanliness is also of paramount importance in getting a sound weld. Poor cleanliness can lead to increased porosity. Therefore, both the workpiece and the filler metal were thoroughly cleaned as described earlier, and the butting edges were given a light acid etch prior to welding to remove any oxide layer that may have been present on the surface. The optimized parameters given in Table 1 together with a good cleaning procedure can give radiographically sound joints in Ti-6Al-4V sheet as per the ASME pressure vessel code (Ref. 3).

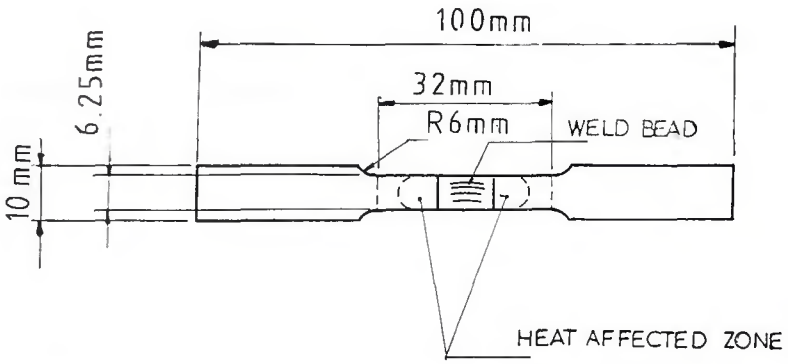

Fig. 2 — Smooth tensile specimen used for testing GTA welds.

Microstructure

The microstructure of the base metal shown in Fig. 3 consists of fairly equiaxed alpha grains with beta at the alpha grain boundaries. The FZ microstructures of Samples A, C and D are almost similar, containing acicular and serrated types of alpha in large prior beta grains. Figure 4 shows the microstructure of the FZ of Sample A. The microstructure (Fig. 5) of the FZ of Sample B consists predominantly of fine acicular alpha, which accounts for the high ductility of the weld sample. The FZ microstructure of sample E (Fig. 6) reveals the presence of a large number of wide serrated alpha plates and small quantities of retained beta.

The microstructure of the HAZ of all the samples contained small quantities of primary alpha, serrated alpha, acicular alpha and transformed beta. Figure 7 shows the microstructure of the HAZ of Sample E.

Hardness Evaluation

The hardness measurements made across the BM, HAZ and FZ, are plotted against distance from the center of the FZ as shown in Fig. 8. The hardness variation across the weldment depends on the type, quantity and distribution of the transformation products (Ref. 4). However, in this investigation, no quantitative measurements were made for the various phases present in the microstructure. The solution treatment at 950°C for half an hour followed by aging at 540°C for one hour should yield a hardness (Ref. 5) of 40 RC. The relatively low hardness obtained in the present experiments was attributed to the slow quenching rate, which resulted from the poor thermal conductivity of the glass coating over the samples.

From Fig. 8, it was found that the hardness of the HAZ and FZ were more than that of the base metal in all cases with the exception of Sample E where the hardness in the HAZ is lower than that of the base metal. The maximum hardness peaks were found in Samples A and D. The increase in hardness due to stress relieving was expected because of the precipitation of alpha from the small quantities of retained beta in the FZ and HAZ.

Although Sample A was in the annealed state and Sample D was in the solution treated and aged condition, their hardness peaks were seen to coincide on postweld stress relieving. The difference in the heights of the hardness peaks of Samples A and D comes from the basic difference in the hardness of the base metal. It is also evident from Sample D that the increase in hardness, ΔA_1, over Sample E has come exclusively from the subsequent stress relieving operation, and hence, the same hardness component ΔA_1 can be assigned to Sample A as one due also to stress relieving. In the case of Sample E, where welding was the final operation, the increase in hardness, ΔE, over the base metal comes from the weld structure alone. Therefore, in the case of Sample A, the hardness component due to weld structure can be taken as ΔA_2 — the height from the base metal hardness of Sample A to the peak hardness of Sample E. Thus, the height ΔA of the hardness peak of Sample A is made up of two components: ΔA_1 resulting from the stress relieving operation and ΔA_2 resulting from the weld structure.

It is interesting to note in the case of Sample B that there was no variation in hardness across the base metal, the HAZ and the FZ. This homogenization in hardness must have resulted from the solution treatment and aging operation carried out subsequent to welding. In the case of Sample C, the increase in hardness ΔC_1 over Sample E has come purely from the subsequent aging treatment. It may also be seen that ΔC_1 is less than ΔA_1. This must have resulted from

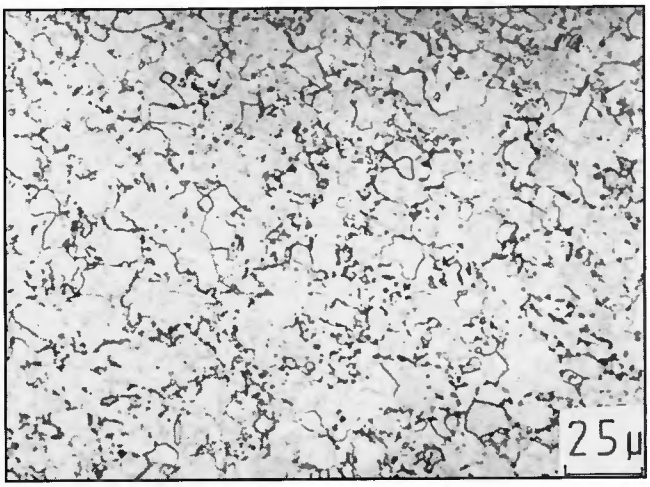

Fig. 3 — Microstructure of annealed base metal.

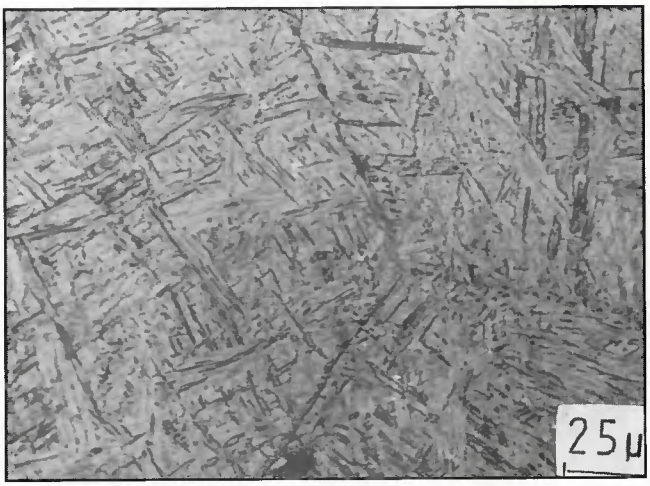

Fig. 4 — Fusion zone microstructure of Sample A.

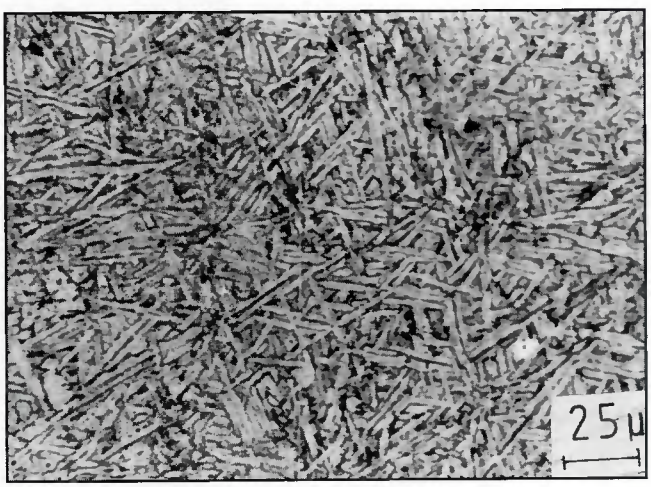

Fig. 5 — Fusion zone microstructure of Sample B.

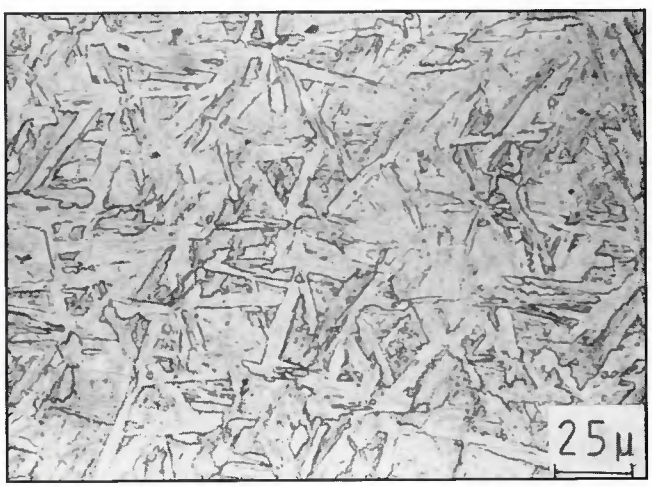

Fig. 6 — Fusion zone microstructure of Sample E.

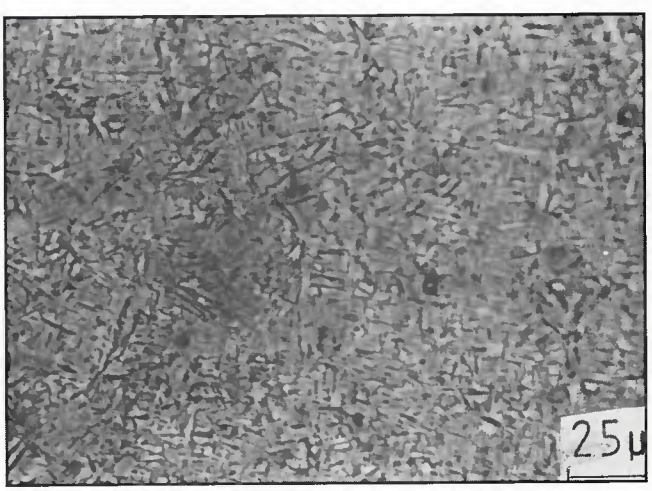

Fig. 7 — Heat-affected zone microstructure of Sample A.

the greater extent of aging taking place at the higher stress relieving temperature (Ref.6). The HAZ of Sample E shows hardness values slightly lower than those of the base metal. This decrease in hardness in the HAZ is attributed to the final welding operation wherein regions of the HAZ close to the FZ have been raised to temperatures above the solutionizing temperature and regions of the HAZ close to the base metal to temperatures above the overaging temperature.

Table 2— Mechanical Properties of Base Metal and Welded Samples

Group	Condition	Fracture Location	UTS (MPa)	0.2% YS (MPa)	% Elongation
O	Annealed base metal	—	883	794	14.0
S	Solution treated and aged base metal	—	1020	932	10.5
A	Annealed samples welded and then stress relieved	BM	892	824	4.8
B	Annealed samples welded and then solution treated and aged.	FZ	1010	892	8.0
C	Solution treated samples welded and then aged	BM	1020	902	5.2
D	Solution treated & aged samples welded and then stress relieved	BM	981	92	5.8
E	Solution treated and aged samples welded	HAZ	942	892	4.0

Mechanical Properties

Mechanical properties of the welded samples subjected to different preweld and postweld heat treatments, as well as those of the base metal in the annealed and in the solution treated and aged conditions, are tabulated in Table 2. Although the ultimate tensile strength (UTS) and yield strength (YS) of the samples of condition A are not affected, the percentage of elongation (%E) is only 4.8 vs. 14 for the base metal. Sample B, which was subjected to a postweld solution treatment and aging operation, showed UTS, YS and %E values comparable to those of the base metal in the same condition. Figure 8 shows no hardness variation across the BM, HAZ and FZ of Sample B, and the tensile fracture was located in the FZ. During tensile testing, the BM, HAZ and FZ of Sample B underwent more or less uniform straining, and it exhibited the maximum ductility of all the welded samples. The tensile ductility of samples belonging to conditions C, D and E are poor like that of Sample A. The high rate of heat input to the samples, when compared to the electron beam welding process, gives a FZ of 15 to 20 mm (0.6 to 0.8 in.) width. Consequently, the cooling rate of the FZ is relatively low and the resulting microstructure in the FZ of Sample E (Fig.6) does not reveal the presence of any martensite but only serrated alpha. This alpha phase does not undergo any noticeable change in the subsequent stress relieving or aging operations, as seen in the microstructure of Sample A — Fig. 4.

As the molten weld pool cooled down through the alpha and beta region, the vanadium content of the beta phase kept increasing and the martensite start (MS) and martensite finish (MF) temperatures progressively decreased. It is reported (Ref. 7) that at a temperature of 840°C (1544°F) the MF temperature of Ti-6Al-4V is less than 25°C (77°F). The FZ is therefore likely to contain small quantities of retained beta or metastable beta phase. During the postweld stress relieving or aging operation, the metastable beta gave rise to precipitation of fine alpha, which cannot be seen under an ordinary microscope. This precipitation makes the FZs of Samples A, C and D much harder than the BM, as seen in Fig. 8. As a result, during tensile testing, the BM, HAZ and FZ across the gauge length underwent nonuniform deformation. The BM, being softer than the other zones, experienced larger localized strains, and the fracture of the specimen took place in this zone. The UTS and YS of samples for conditions A, C and D, therefore, remain almost on the same level as the base metal for the respective conditions.

In the case of Sample E, the tensile fracture occurred in the HAZ. During

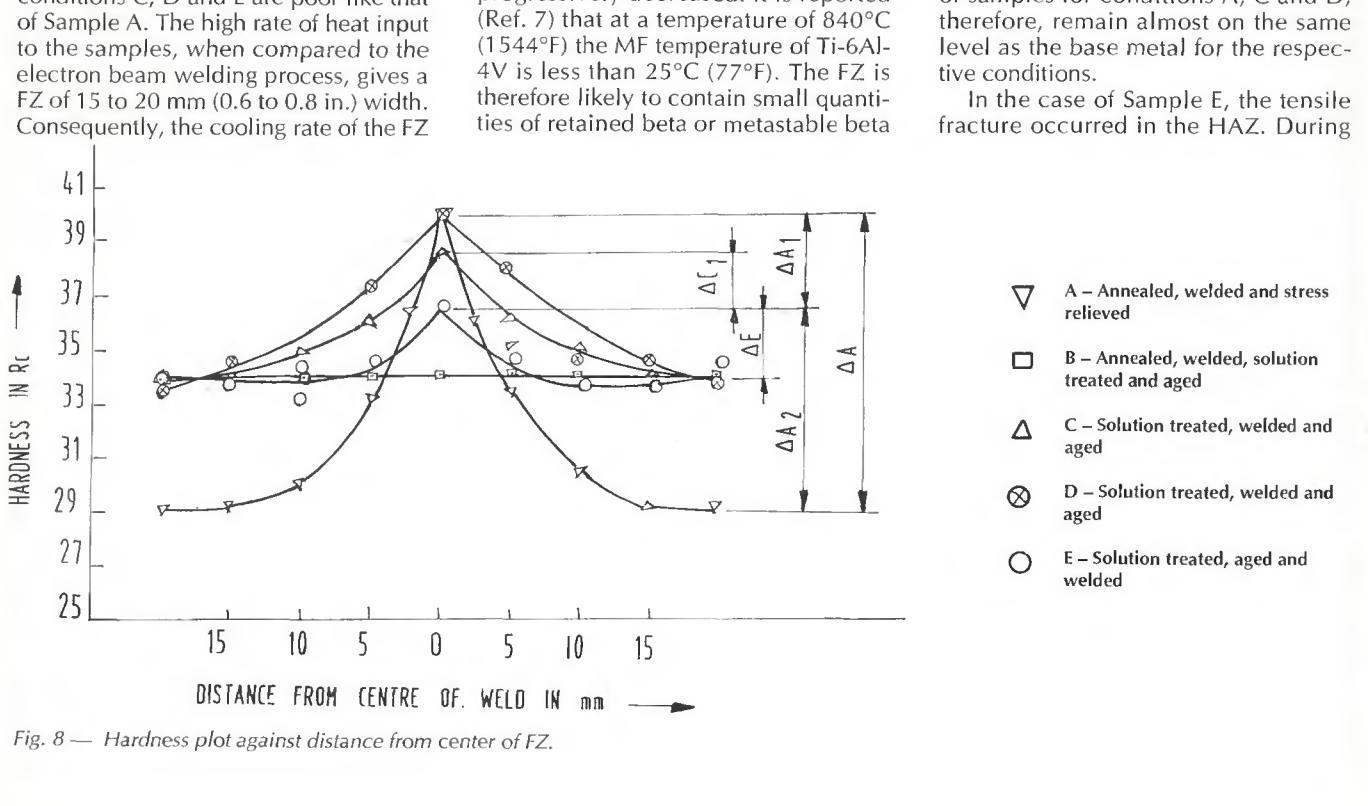

Fig. 8 — Hardness plot against distance from center of FZ.

the final welding operation of Sample E, the HAZ became softer (Fig. 8) than the other zones. This led to strain concentration in this zone during tensile testing, and the fracture took place at the HAZ. It can also be seen that the UTS and YS of Sample E are lower than those of the base metal in condition S.

In the case of 0.6-mm-thick Ti-6Al-4V sheet, Borggreen and Wilson (Ref. 8) have reported a tensile ductility of 2.5% in the GTA as-welded condition. Improving the as-welded ductility to 6.8% compared to the base metal value of 9.2% could be done by resorting to a triplex heat treatment. In the present investigation, it was found that the weld ductility can be subsequently improved by a postweld solution treatment and aging operation. The weld ductility of Sample B increased to 100% over Sample E and to 80% of the base metal of condition S.

Conclusions

I) The optimum welding schedule given in Table 1 can yield a radiographically sound weld in 2.6-mm-thick Ti-6Al-4V sheet.

2) The presence of large quantities of coarse serrated alpha phase in the FZ has a deleterious effect on the weld ductility compared to the fine acicular alpha phase of the postweld solution treated and aged sample or the equiaxed alpha phase of the base metal in annealed condition.

3) Low temperature postweld heat treatments, like stress relieving, do not have any appreciable effect in improving the ductility of the as-welded samples.

4) The high hardness of the FZ results from the stress relieving/aging operation and the weld structure.

5) The contribution to FZ hardness by stress relieving is more than that by the weld structure in the case of solution treated and aged base metal.

6) In the case of annealed base metal, the contribution to FZ hardness by the weld structure is appreciable.

7) Weld ductility of the as-welded sample could be 100% improved by subjecting it to a solutionizing and aging treatment.

8) The combination of preweld solutionizing treatment followed by postweld aging gives UTS and YS values almost equal to the base metal in the solution treated and aged condition but at 50% of its ductility.

Acknowledgments

The authors wish to acknowledge the support rendered by the welding and heat treatment, and the metallography and fabrication sections of the Materials and Metallurgy Group toward the completion of this investigation. They are also indebted to Shri D. Easwardas, deputy director, Materials and Mechanical Systems, for his constant encouragement and guidance. They also extend their gratitude to Dr. S. C. Gupta, director, VSSC, for permission to publish this work.

References

1. Thomas, G., and Mukherjee, M. K. 1975. Role of titanium in aerospace applications, J. of Aero. Society of India, p. 11.

2. Woolcock, A. 1982. The effect of welding speed and edge preparation on the incidence of porosity in TIG welded titanium. *Titanium and Titanium Alloys, Scientific and Technological Aspects,* Vol. 2, J. O.Williams and A. F. Belov, eds., Plenum Press, p.1189.

3. ASME *Boiler and Pressure Vessel Code,* Section 8, Part UW, American Society of Mechanical Engineers, New York, N.Y., p. 79.

4. Stubington, C. A., and Ballet, J. T. 1973. Weld optimization and fracture tests in low-voltage electron beam welded 2-in.-thick Ti-6A1-4V alloy. *Titanium Science and Technology,* Vol. 1, R. I. Jaffee and H. M. Burte, eds., Plenum Press, p.601.

5. Fopiano, P. J., *et al.* 1969. Phase transformations and strengthening mechanisms in the Alloy Ti-6Al-4V. Trans. of ASM, Vol.62, p.324.

6. Maykuth, D. J., *et al.* 1970. Titanium base alloys. *Processing and Properties Handbook,* DMIC, Battelle Memorial Institute, Ohio.

7. Fopiano, P. J., Bever, M. B., and Averbach, B. L. 1969. Phase transformations during the heat treatment of the Alloy Ti-6Al-4V. Trans. of ASM, Vol. 62, p. 324.

8. Borggreen, K., and Wilson, I. 1980. Use of postweld heat treatment to improve ductility in thin sheets of Ti-6Al-4V. *Welding Journal* 59(1):16.